Spectrochimica Acta Part A: Molecular and Biomolecular Spectroscopy 97 (2012) 435–448

Contents lists available at SciVerse ScienceDirect

Spectrochimica Acta Part A: Molecular and Biomolecular Spectroscopy

journal homepage: www.elsevier.com/locate/saa

Synthesis, spectroscopic characterization and quantum chemical computational studies of (*S*)-*N*-benzyl-1-phenyl-5-(pyridin-2-yl)-pent-4-yn-2-amine

Etem Kose [a,*], Ahmet Atac [a], Mehmet Karabacak [b], Caglar Karaca [a], Mustafa Eskici [c], Abdullah Karanfil [c]

[a] Department of Physics, Celal Bayar University, Manisa, Turkey
[b] Department of Physics, Afyon Kocatepe University, Afyonkarahisar, Turkey
[c] Department of Chemistry, Celal Bayar University, Manisa, Turkey

HIGHLIGHTS

- Spectroscopic properties of the new molecule were examined by FT-IR, NMR and UV techniques and DFT.
- The complete assignments are performed on the basis of the total energy distribution (TED).
- Nonlinear optical properties of the molecule were studied.
- HOMO and LUMO energies, molecular electrostatic potential distribution of the molecule was calculated.

GRAPHICAL ABSTRACT

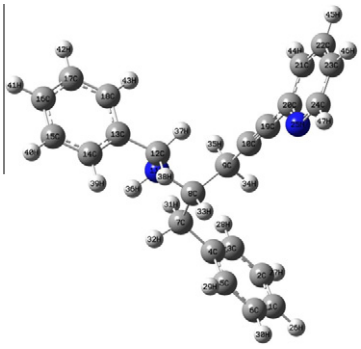

ARTICLE INFO

Article history:
Received 19 April 2012
Received in revised form 3 June 2012
Accepted 25 June 2012
Available online 3 July 2012

Keywords:
DFT
FT-IR
NMR
UV
Nonlinear optics

ABSTRACT

The synthesis and characterization of a novel compound (*S*)-*N*-benzyl-1-phenyl-5-(pyridin-2-yl)-pent-4-yn-2-amine (abbreviated as BPPPYA) was presented in this study. The spectroscopic properties of the compound were investigated by FT-IR, NMR and UV spectroscopy experimentally and theoretically. The molecular geometry and vibrational frequencies of the BPPPYA in the ground state were calculated by using density functional theory (DFT) B3LYP method invoking 6-311++G(d,p) basis set. The geometry of the BPPPYA was fully optimized, vibrational spectra were calculated and fundamental vibrations were assigned on the basis of the total energy distribution (TED) of the vibrational modes, calculated with scaled quantum mechanics (SQM) method and PQS program. The results of the energy and oscillator strength calculated by time-dependent density functional theory (TD-DFT) and CIS approach complement with the experimental findings. Total and partial density of state (TDOS and PDOS) and also overlap population density of state (COOP or OPDOS) diagrams analysis were presented. The theoretical NMR chemical shifts (^{1}H and ^{13}C) complement with experimentally measured ones. The dipole moment, linear polarizability and first hyperpolarizability values were also computed. The linear polarizabilities and first hyper polarizabilities of the studied molecule indicate that the compound is a good candidate of nonlinear optical materials. The calculated vibrational wavenumbers, absorption wavelengths and chemical shifts showed the best agreement with the experimental results.

Introduction

The phenyl and pyridine groups are found together in many organic compounds, both natural and synthetic products [1,2] and their derivatives (especially for pyridine) are very important in industrial field as well as in biochemistry, showing interesting photo chemical and electrochemical properties [3–6]. Many substituted pyridines are involved in bioactivities with applications in pharmaceutical drugs and agricultural products [7–9].

The density functional theory (DFT) has emerged as a powerful tool in studying vibrational spectra of fairly large molecules. The

* Corresponding author. Tel.: +90 236 241 2151x2566.
E-mail address: etemmm43@gmail.com (E. Kose).

1386-1425/$ - see front matter © 2012 Elsevier B.V. All rights reserved.
http://dx.doi.org/10.1016/j.saa.2012.06.041

DFT calculations are reported to provide excellent vibrational frequencies of organic compounds if the calculated frequencies are scaled to compensate for the approximate treatment of electron correlation [10–12]. The calculations based on DFT have been applied in many areas, and the results are also in great agreement with the experimental results in calculating vibrational frequencies [13–15]. The vibrational and theoretical studies of the phenyl and pyridine ring systems were reported by several investigations [16–20].

The GIAO method is one of the most common approaches for calculating nuclear magnetic shielding tensors. The GIAO approach allows the computation of the absolute chemical shielding due to the electronic environment of the individual nuclei and this method is often more accurate than those calculated with other approaches for the same basis set. DFT/GIAO approach is widely used for the calculations of chemical shifts for a variety of heterocyclic compounds [21–24].

As a part of research program aimed at investigation of reactivity of cyclic sulfamidates towards acetylides, BPPPYA using the reaction of phenylalanine-derived 1,2-cyclic sulfamidate with the acetylide prepared from 2-ethynylpyridine is synthesized [25]. The aim of this study is to present a detailed description of the molecular geometry, vibrational frequencies, and energies of optimized structures and chemical shifts of the title compound for the first time using both computational and experimental techniques (FT-IR, ^{13}C and ^{1}H NMR and UV–Vis spectra). We have utilized the gradient corrected density functional theory (DFT) [26] with the Becke's three-parameter hybrid functional (B3) [27] for the exchange part and the Lee–Yang–Parr (LYP) correlation function [28], accepted as a cost-effective approach, for the computation of molecular structure, vibrational frequencies and energies of optimized structures. In this context, in the ground state theoretical geometric parameters, IR, NMR and UV spectra, HOMO and LUMO energies of title molecule were calculated by using Gaussian 09 suite of quantum chemical codes [29], for the first time. All results which examined by the experimental techniques (IR, NMR and UV spectra) were compared with computed results. Calculated vibrational wavenumbers, absorption wavelengths and chemical shift values are in fairly good agreement with the experimental results. Besides, the dipole moment, linear polarizability and first hyperpolarizability, chemical hardness, electronegativity, chemical potential, electrophilicity index and Mulliken atomic charges were also studied using the B3LYP/6-311++G(d,p) basis set.

Materials and methods

Materials

Hexamethylphosphoramide (HMPA) was distilled from sodium metal and tetrahydrofuran (THF) was freshly distilled from $LiAlH_4$ before use. 2-Ethynylpyridine was purchased from Aldrich Chemical Company (USA) and used as received. (*S*)-3,4-Dibenzyl-1,2,3-oxathiazlodine-2-2-dioxide was prepared according to literature procedure [30].

Synthesis of (S)-N-benzyl-1-phenyl-5-(pyridin-2-yl)-pent-4-yn-2-amine

To a stirred solution of 2-ethynylpyridine (438 mg, 4.59 mmol) in 15 mL freshly distilled dry THF containing 1.5 mL HMPA cooled at −78 °C (dry ice-acetone) under argon atmosphere was added dropwise *n*-butyllithium (2.9 mL, 4.62 mmol, 15% solution in *n*-hexane). After stirring at −78 °C for 1 h, a solution of (4*S*)-3,4-dibenzyl [1–3]oxathiazolidine-2,2-dioxide (700 mg, 2.29 mmol) in 3 mL dry THF was added to the resulting acetylide solution via a syringe and stirring continued for additional 8 h at −78 °C. The reaction mixture was allowed to warm up to room temperature gradually with stirring overnight (24 h). The resulting mixture was then treated with 5 M 3 mL HCl solution to hydrolyze the *N*-sulfate intermediate for 2 h before neutralization with saturated $NaHCO_3$ solution. Extraction with ether three times and drying over anhydrous Na_2SO_4 followed by evaporation of volatiles *in vacuo* gave the crude product. Purification by column chromatography using a (EtOAc: hexane (1:4) to (1:1) gradient) solvent system containing 0.5% triethylamine afforded (*S*)-*N*-benzyl-1-phenyl-5-(pyridin-2-yl)pent-4-yn-2-amine as a dark yellow oil (537 mg, 71% yield). Partial decomposition of the alkynlated amine product on silica was also observed. R_f: 0.61 [(EtOAc: hexane) 1:1]; $[\alpha]_D^{31}$ + 4.2 (c = 1, $CHCl_3$); IR (film); υ_{max}/cm^{-1} 3322 (NH), 2227 (C≡C), 1603,1584, 1562, 1494, 1465, 780, 738, 699 (aromatic ring); δ_H (400 MHz, $CDCl_3$) (ppm) 2.56 (1H, $\delta\delta$, J = 5.2 and 17), 2.62 (1H, $\delta\delta$, J = 5.2 and 17), 2.91 (1H, $\delta\delta$, J = 7.2 and 13.6), 2.96 (1H, $\delta\delta$, J = 6.8 and 13.6), 3.07–3.13 (1H, m), 3.82 (1H, δ, J = 13.2), 3.92 (1H, δ, J = 13.2), 7.18–7.30 (11H, m, Ar—H), 7.39 (1H, δ, J = 8, Ar—H), 7.62 (1H, $\tau\delta$, J = 0.4 ve 7.6, Ar—H), 8.56 (1H, δ, J = 5.2, Ar—H); δ_C (100 MHz, $CDCl_3$) (ppm) 24.31, 40.74, 51.36, 57.30, 82.87, 88.08, 122.68, 126.59, 127.12, 127.19, 128.25, 128.59, 128.68, 129.62, 136.25, 138.98, 140.43, 143.93, 150.10. HRMS (CI): $[M+H]^+$ found 327.1861, $C_{23}H_{23}N_2$ requires 327.1861 (Scheme 1).

Experimental details

The FT-IR spectrum of the BPPPYA was recorded in the region 600–4000 cm^{-1} on a Perkin-Elmer FT-IR System Spectrum BX spectrometer which was calibrated using polystyrene bands and under 400 cm^{-1} on Bruker IFS 66/S. The ultraviolet absorption spectrum of the BPPPYA, solved in ethanol, was examined in the range 190–800 nm using Shimadzu UV-1700 PC, UV–vis recording Spectrophotometer. NMR experiments were performed in Varian Unity AS 400 spectrometer at 300 K. Chemical shifts were reported in ppm relative to tetramethylsilane (TMS) for ^{1}H and ^{13}C NMR spectra. The compound was dissolved in chloroform ($CDCl_3$). ^{1}H and ^{13}C NMR spectra were obtained at a base frequency of 100 MHz for ^{13}C and 400 MHz for ^{1}H nuclei.

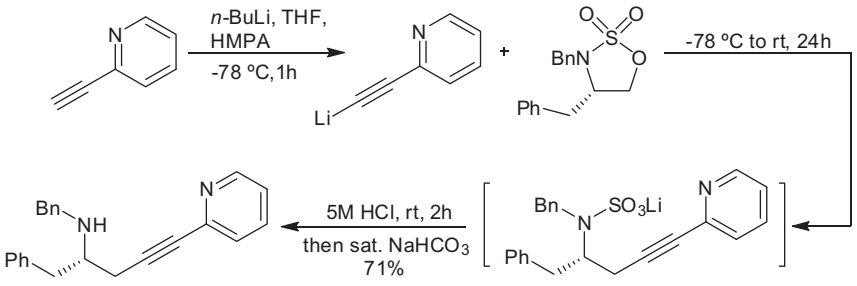

Scheme 1. Synthesis of (*S*)-*N*-benzyl-1-phenyl-5-(pyridin-2-Yl)-pent-4-yn-2-amine.

Quantum chemical calculations

The molecular structure of the BPPPYA in the ground state is optimized using DFT levels on a personal computer using Gaussian 09 [29] program package, invoking gradient geometry optimization [31]. Based on our previous experience [32–34] this method and the fairly large and flexible basis set 6-311++G(d,p) level were chosen to perform accurate calculations on the title molecule. Optimized structural parameters were used in the vibrational frequency, isotropic chemical shift and calculations of electronic properties. The vibrational frequencies in the ranges from 4000 to 1700 cm^{-1} and lower than 1700 cm^{-1} are scaled with 0.958 and 0.983, respectively, in order to improve the agreement with the experimental results [12]. The complete vibrational assignments were performed on the basis of the total energy distribution (TED) of the vibrational modes, using the scaled quantum mechanical (SQM) method and PQS program [11,35]. For NMR calculations, after optimization, ^{1}H and ^{13}C NMR chemical shifts were calculated using the gauge-invariant atomic orbital (GIAO) method [36,37] in chloroform. The electronic properties, such as HOMO–LUMO energies, absorption wavelengths, and oscillator strengths were calculated by CIS approach and using B3LYP method of the time-dependent DFT (TD-DFT) [29,38,39], based on the optimized structure. The CIS method gives more accurate results [40] than the using B3LYP method of the time-dependent DFT (TD-DFT). Hence we used the results of CIS approach for the electronic properties. Obtained wavelengths λ_{max} were compared with the experimental UV absorption of the BPPPYA.

Results and discussion

Geometrical structure

The title molecule consists of three rings (two phenyl and one pyridine ring). The optimized geometric structure (with *x* and *y* position) of the BPPPYA is given in Fig. 1 with numbering of the atoms. The optimized bond lengths, bond angles, and selected dihedral angles of the BPPPYA calculated using DFT/B3LYP/6-311++G(d,p) are listed in Table 1 in accordance with numbering given in Fig. 1.

The phenyl rings and pyridine ring are coplanar with the each other, but all groups are non-planar therefore C_1 point group symmetry is used for computation. The optimized bond lengths of C—C in the phenyl ring fall in the range from 1.393 to 1.402 Å for B3LYP/6-311++G(d,p) methods which are in good agreement with those of structurally similar systems whose crystal structures are elucidated (1.371–1.402 Å) [41–43]. The optimized C—N bond lengths are calculated between 1.471 and 1.475 Å and show good coherent with the observed value of 1.46 Å for structurally similar structure [36]. The bond angles in phenyl and pyridine rings of the BPPPYA are in a good agreement with similar structures. For example, the calculated average of C—C—C groups in the phenyl rings are 120.1° and 119.8° and the computed average values of same angles in pyridine ring are 119.2°, show good agreement in 120° expected value.

Vibrational analysis

The objective of the vibrational analysis is to find vibrational modes connected with molecular structure of the novel compound under scrutiny. The numerical harmonic vibrational analysis was done for the optimized geometry of BPPPYA, under assumption C_1 point group symmetry. Vibrational spectral assignments were performed on the recorded FT-IR spectrum and theoretically predicted wavenumbers and their TED. The studied molecule consists of 47 atoms therefore they have 135 vibrational normal modes. The experimental and calculated frequencies and their assignments with TED of the title compound are given in Table 2 and Table S1 (Supp. Mat.). The calculated and observed IR spectra are shown in Fig. 2, where the calculated intensity is plotted against the harmonic vibrational wavenumbers. DFT potential symmetrically overestimates the vibrational wavenumbers. These discrepancies are corrected either by computing anharmonic corrections explicitly or by introducing a scaled field or by directly scaling the calculated wavenumbers with a proper factor. Considering systematic errors, we scaled the vibrational wavenumbers calculated by B3LYP method with two scaling factors of 0.983 up to 1700 cm^{-1} and 0.958 for greater than 1700 cm^{-1} [12]. After wavenumbers ordered with the scaling factors, the calculated vibrational wavenumbers showed very good concinnity with the experimental values. The vibrational analysis of title compound was performed on the basis of the characteristic vibrations of C—H, C—C, C=C, NH, C—N, C≡C, pyridine and phenyl ring modes.

C—H vibrations

The hetero-aromatic structures show the presence of C—H stretching vibration in the region 3100–3000 cm^{-1}, which is the characteristic region for the ready identification of C—H stretching vibration [44–46]. The existence of one or more aromatic rings in a structure is normally readily determined from the C—H and C≡C—C related vibrations. The C—H stretching vibration occurs above 3000 cm^{-1} and is typically exhibited as a multiplicity of weak to moderate bands, compared with the aliphatic C—H stretch [43]. In our study three peaks were obtained at 3020, 3026 and 3062 cm^{-1} in FT-IR spectrum which assigned to C—H stretching vibration of the rings. However, C—H stretching modes due to the fourteen adjacent hydrogen atoms around the three rings, were predicted in the range of 3023–3070 cm^{-1} (see Supp. Mat. Table S1, modes $\nu 2$–$\nu 15$) by quantum chemical calculations. As indicated by TED, these modes shows >98% contribution, suggested pure stretching modes.

The in-plane C—H bending vibrations appear in the range 1000–1300 cm^{-1} and the C—H out of plane bending vibrations occur in the frequency range 750–1000 cm^{-1}. In this study, the C—H in plane and out-of-plane bending vibrations lie within the characteristic region. For example, the C—H in-plane bending vibration is observed at 1174 cm^{-1} in FT-IR for phenyl rings. The calculated frequency at 1175 cm^{-1} is very well correlated with the experimental frequency. The C—H out of plane bending vibrations were predicted in the region of 988–780 cm^{-1} for phenyl rings. The observed frequencies (988, 912 and 845 cm^{-1}) are coinciding very well with the calculated ones (991, 918 and 845 cm^{-1}, respectively).

The C—H out of plane bending of the pyridine ring were calculated at 784, 894 and 970 cm^{-1} and found to be in good agreement with observed values at 780, 892 and 968 cm^{-1} in FT-IR. According to TED, the CH in plane bending modes of pyridine ring were predicted at 1152 and 1096 which had major contribution (78% and 39%, respectively). These mode were observed at 1150 and 1092 cm^{-1}. All aromatic C—H bands show good coherent with experimental values and literatures.

CH_2 vibrations

The C—H stretching of the methylene groups are at lower frequencies than those of the aromatic C—H ring stretching. The symmetric stretching for the CH_2, CH_3, etc. has magnitude lower than the asymmetric stretching. The CH_2 anti-symmetric stretching modes are generally observed in the region 3000–2900 cm^{-1}, while the CH_2 symmetric stretching modes will appear between 2900 and 2800 cm^{-1} [31,38,47]. In this work, the CH_2 asymmetric and symmetric stretching vibrations were observed in FT-IR

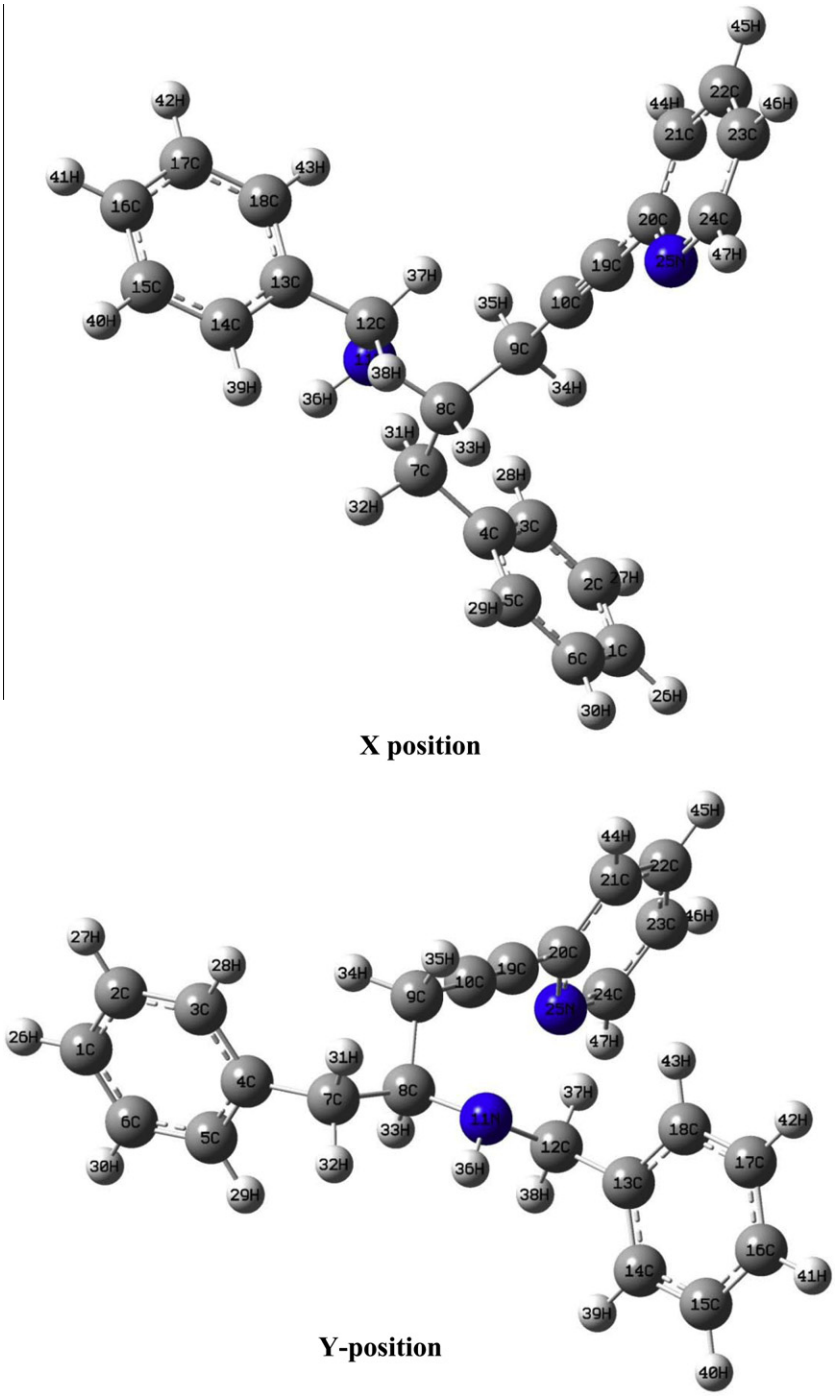

Fig. 1. The theoretical optimized geometric structure and atoms numbering of BPPPYA for two positions.

spectra at 2925 and 2849 cm^{-1}, respectively, and the calculated asymmetric CH_2 stretching vibrations of the methylene group were obtained at 2958, 2938, 2931 and the calculated symmetric ones were obtained at 2897, 2894 and 2831 cm^{-1}. The scissoring mode of the CH_2 group gives rise to characteristic bands near 1465 cm^{-1} in IR spectrum [48]. The CH_2 scissoring vibrations were calculated at 1463, 1429 and 1427 cm^{-1}. The experimental value was assigned at 1427 cm^{-1} which show excellent agreement with calculated one which had major contribution according to TED (90%). The other CH_2 vibrations, wagging, twisting and rocking mode, were calculated at 1374 and 1289 cm^{-1}, 1237, 1212 and 1176 cm^{-1}, 972 and 882 cm^{-1}, respectively.

CC ring vibrations

The ring stretching vibrations are important in the spectrum of pyridine and its derivatives, are highly characteristic of the aromatic ring itself. The aromatic ring carbon–carbon stretching vibrations occur in the region 1430–1625 cm^{-1}. In general, the bands are of variable intensity and are observed at 1625–1590, 1575–1590, 1470–1540, 1430–1465 and 1280–1380 cm^{-1} from the frequency ranges given by Varsanyi [49] for the five bands in the region. In the present work, C—C stretching vibrations computed between 1050 and 1591 cm^{-1} for pyridine and between 998 and 1612 cm^{-1} for phenyl ring, show nice cover with the experimental values.

Table 1
Optimized bond lengths (Å) and bond angles (°) of BPPPYA by using B3LYP/6-311++G(d,p).

Bond lengths (Å)	B3LYP	Bond angels (°)	B3LYP
Parameters			
C1—C2	1.394	C2—C1—C6	119.5
C1—C6	1.396	C1—C2—C3	120.1
C2—C3	1.396	C2—C3—C4	121.0
C3—C4	1.400	C3—C4—C5	118.2
C4—C5	1.402	C3—C4—C7	121.1
C4—C7	1.513	C5—C4—C7	120.7
C5—C6	1.394	C4—C5—C6	121.0
C7—C8	1.546	C1—C6—C5	120.2
C8—C9	1.551	C4—C7—C8	114.9
C8—N11	1.471	C4—C7—H31	109.9
C8—H33	1.101	C4—C7—H32	108.9
C9—C10	1.459	C8—C7—H31	108.6
C10—C19	1.209	C8—C7—H32	107.5
N11—C12	1.475	C7—C8—C9	109.9
N11—H36	1.016	C7—C8—N11	107.9
C12—C13	1.512	C7—C8—H33	108.2
C13—C14	1.399	C9—C8—N11	111.5
C13—C18	1.401	C9—C8—H33	108.1
C14—C15	1.396	N11—C8—H33	111.0
C15—C16	1.394	C8—C9—C10	116.1
C16—C17	1.397	C8—C9—H34	108.2
C17—C18	1.393	C8—C9—H35	108.2
C19—C20	1.432	C10—C9—H34	107.5
C20—C21	1.404	C10—C9—H35	109.7
C20—N25	1.350	C8—N11—C12	115.6
C21—C22	1.389	C8—N11—H36	108.3
C22—C23	1.393	C12—N11—H36	107.7
C23—C24	1.394	N11—C12—C13	110.7
C24—N25	1.336	N11—C12—H37	108.4
C—H phenyl ring (average)	1.085	N11—C12—H38	111.6
C—H pyridine ring (average)	1.084	C13—C12—H37	109.6
C—H methylene (average)	1.096	C13—C12—H38	109.4
Bond angels (°)		C12—C13—C14	120.8
C19—C20—C21	120.3	C12—C13—C18	120.6
C19—C20—N25	117.4	C13—C18—C17	120.8
C21—C20—N25	122.3	C13—C14—C18	118.6
C20—C21—C22	118.9	C13—C14—C15	120.8
C21—C22—C23	118.9	C14—C15—C16	120.0
C22—C23—C24	118.2	C15—C16—C17	119.6
C23—C24—N25	123.8	C—C—H (phenyl ring) average	119.8
N25—C24—H47	116.0	C—C—H (pyridine ring) average	120.6
C20—N25—C24	117.8	H—C—H (methylene) average	106.8
C16—C17—C18	120.1		

The CCC in plane deformation vibrations are at higher wavenumbers than the CCC out of plane vibrations. The theoretically calculated in-plane and out-of plane vibrations show good agreement with recorded spectral data. The ring deformation, torsion and CCC bending modes contaminated with other modes and missing in FT-IR spectrum (except ν103–104 and ν119). The ring deformation, torsion and out-of-plane CCC bending modes are obtained in a large region like vibrational modes of the BPPPYA. Also the TEDs of these vibrations are not pure modes as it is evident from the last columns of (Table 1 and Table S1).

The ring breathing vibrations are observed in the region 1100–1000 cm^{-1}. As revealed by TED, the ring-breathing mode of the aromatic rings at 998 cm^{-1} for phenyl ring and 980 cm^{-1} for pyridine ring (Supp. Mat. Table S1). The ring assignments proposed in this study are also in agreement with literature values [23,45,50].

N—H Vibrations

It is stated that the N—H stretching vibrations; in primary aliphatic amines occur in the region 3300–3500 cm^{-1}, and in secondary aliphatic amines frequency falls in the range 3310–3360 with low intensity [51]. In previous work N—H symmetric stretch in primary aliphatic amine was computed at 3470 cm^{-1} and experimental value was observed at 3274 cm^{-1} in FT-IR [34]. Now the NH stretching vibration in secondary aliphatic amine computed at 3353 cm^{-1} (ν1) by B3LYP method and recorded only one band at 3322 cm^{-1} in FT-IR. This mode is a pure mode as is evident from TED column contributing exactly 100%.

CN vibrations

The CN stretching frequency is a rather difficult task since there are problems in identifying these frequencies from other vibrations. Colthup [52] indicted correlations for aliphatic amines with absorptions in 1120–1020 cm^{-1} range. These correlations were confirmed and extended by Stewart [53] by measurements on numbers of primary and secondary amines. In this study, CN stretching vibrations of secondary amine were computed at 804–1097 cm^{-1} and observed only at 1008 cm^{-1} in FT-IR spectra. The CN vibrations usually mixed with other vibrations. The TED results show that this vibration contaminated with C—C stretching vibration. It is worth mentioning that, ν62 mode the highest contribute for this vibration at about 1104 cm^{-1} is not combined with other modes.

As the CN modes in pyridine rings; Sundaraganesan [15] assigned CN stretching absorption in the region 1381 cm^{-1} for 2-amino-5-iodopyridine. In the previous work, the band observed at 1374 cm^{-1} in FT-IR spectrum (1376 cm^{-1} in FT-Raman) and computed at 1371 cm^{-1}, assigned to CN stretching vibration for 6-chloronicotinic acid [54]. Kumar et al. [55] have calculated the frequency for the C—N stretching mode falls in the region 1350–1370 cm^{-1} for both nicotinamide and its N-oxide with strong IR intensity. Also, in previous work, TED of C—N stretching is contributing 41% and 42% to the modes were predicted at 1264 and 1274 cm^{-1} and observed at 1272/1268 cm^{-1} (IR/Ra) and 1258 cm^{-1} (IR) for 2/6-bromonicotinic acid, respectively [34]. For the BPPPYA, the C═N stretching vibration of pyridine was computed at 1104 cm^{-1} and at 1115 cm^{-1} in FT-IR spectrum. Theoretically computed value of CN stretching vibrations show good correlations with experimental values.

C≡C vibrations

The C≡C modes, its position is highly characteristic, arise from conjugation and from aromatic substations are also very informative. In symmetrical structures the C≡C absorption is often too weak to be detectable, and in these circumstances there is no sure way of recognizing this type of bond, other than by the corresponding Raman spectrum. The C≡C vibrations were observed in the region 2235–2260 cm^{-1} by Allan et al. [56]. In our work, the C≡C absorption band was observed at 2227 cm^{-1} in FT-IR. This mode coupled with the CC stretching was calculated at 2221 cm^{-1} proved with the TED value contributing to 83%. Also this mode is very good agreement with given by Bellamy [57].

The correlation graphic which described harmony between the calculated and experimental wavenumbers (Fig. 3). As can be seen from Fig. 3, experimental fundamentals have a good correlation with B3LYP. The relations between the calculated and experimental wavenumbers are linear and described by the following equation:

$$\upsilon_{cal.} = 1.0014\upsilon_{exp.} - 0.2618 \quad (R^2 = 0.9999)$$

As a result, the scaled fundamental vibrational are in good consistency with the experimental results and are found a good agreement above the predicated literature.

UV spectrum and electronic properties

The UV spectrum of the BPPPYA was taken in ethanol solution and also calculated with by CIS approach as this method produced

Table 2
Selected comparison of the calculated harmonic frequencies using by B3LYP methods 6-311++G(d,p) and experimental wavenumbers (FT-IR) (cm^{-1}) of BPPPYA.

Modes no.	Exp.	Theoretical		TED[b] (⩾10%)
	FT-IR	Unscaled freq.	Scaled freq.[a]	
ν1	3322	3500	3353	νNH (100)
ν3	3062	3198	3064	νCH $_{\text{pyridine ring}}$ (100)
ν11	3026	3161	3028	νCH $_{\text{phenyl ring}}$ (100)
ν15	3020	3156	3023	νCH $_{\text{pyridine ring}}$ (97)
ν18	2925	3059	2931	νCH_2 $_{\text{(asymmetric)}}$ (99)
ν21	2849	2955	2831	νCH_2 $_{\text{(symmetric)}}$ (98)
ν23	2227	2318	2221	$\nu C_{19}{\equiv}C_{10}$(90)
ν25	1603	1639	1611	νC—C $_{\text{phenyl ring}}$ (60)
ν28	1584	1618	1590	νC—C $_{\text{phenyl ring}}$ (69) + δCCH $_{\text{phenyl ring}}$ (13)
ν29	1562	1595	1568	νC—C $_{\text{pyridine ring}}$ (56) + νNH (11) + δCCH $_{\text{pyridine ring}}$ (22)
ν31	1494	1524	1498	δCCC $_{\text{phenyl ring}}$ (60) + νC—C $_{\text{phenyl ring}}$ (27)
ν34	1465	1492	1466	δCCH $_{\text{pyridine ring}}$ (51) + νCC $_{\text{pyridine ring}}$ (18)
ν36	1454	1479	1454	δCCH $_{\text{phenyl ring}}$ (38) + νC—C $_{\text{phenyl ring}}$ (18)
ν39	1427	1452	1427	δCH_2(29) {ρ CH_2}(90)
ν41	1356	1379	1355	δCCH $_{\text{phenyl ring}}$ (27) + τCCH $_{\text{phenyl ring}}$ (15)
ν42	1344	1369	1346	δCCH $_{\text{phenyl ring}}$ (25)
ν50	1268	1290	1268	νCC (41) + δCCH(28)
ν54	1200	1227	1206	νC_{13}—CH_2 (38) + νCC $_{\text{phenyl ring}}$ (17) + δCCH $_{\text{phenyl ring}}$ (11)
ν55	1195	1224	1203	νC_4—CH_2 (35) + νCC $_{\text{phenyl ring}}$ (25) + δCCH $_{\text{phenyl ring}}$ (16)
ν58	1174	1195	1175	δCCH (45)
ν61	1150	1171	1152	δCCH $_{\text{pyridine ring}}$ (78) + νCC $_{\text{pyridine ring}}$ (17)
ν62	1115	1123	1104	νCC (27) + νCN (19) + δCCN (14)
ν64	1092	1115	1096	δCCH $_{\text{pyridine ring}}$ (39) + νCC $_{\text{pyridine ring}}$ (36)
ν66	1074	1099	1080	νCC $_{\text{phenyl ring}}$ (41) + δCCH $_{\text{phenyl ring}}$ (37)
ν67	1048	1068	1050	νCC $_{\text{pyridine ring}}$ (61) + δCCH $_{\text{pyridine ring}}$ (22)
ν69	1028	1046	1028	νCC $_{\text{phenyl ring}}$ (48) + δCCH $_{\text{phenyl ring}}$ (23)
ν71	1008	1027	1009	νCC(22) + νCN (15)
ν77	988	1008	991	γ CH phenyl $_{\text{ring}}$ (72))τHCCH (54) + τCCCH (18)}
ν82	968	987	970	γ CH pyridine $_{\text{ring}}$ (87) {τCCCH $_{\text{pyridine ring}}$ (87)}
ν84	912	933	918	γCH $_{\text{phenyl ring}}$ (74) {τCCCH $_{\text{phenyl ring}}$ (40) + τHCCH $_{\text{phenyl ring}}$ (34)}
ν85	892	909	894	γCH pyridine $_{\text{ring}}$ (93) {τCCCH $_{\text{pyridine ring}}$ (65) + τHCCH $_{\text{pyridine ring}}$ (28)}
ν87	845	859	845	γCH $_{\text{phenyl ring}}$ (99) {τCCCH $_{\text{phenyl ring}}$ (82) + τHCCH $_{\text{phenyl ring}}$ (17)}
ν92	780	797	784	γ CH pyridine $_{\text{ring}}$ (80){τCCCH $_{\text{pyridine ring}}$ (48) + τCCCN $_{\text{pyridine ring}}$ (27)}
ν96	738	750	738	νCC (37) + δCCC $_{\text{pyridine ring}}$ (32)
ν99	699	713	701	τCCCH $_{\text{phenyl ring}}$ (44) + τCCCC $_{\text{phenyl ring}}$ (38)
ν100	629	642	631	δCCN $_{\text{pyridine ring}}$ (33) + δCCC $_{\text{pyridine ring}}$ (32) + δCCH $_{\text{pyridine ring}}$ (18)

[a] Wavenumbers in the ranges from 4000 to 1700 cm^{-1} and lower than 1700 cm^{-1} are scaled with 0.958 and 0.983 for B3LYP/6-311++G(d,p) basis set, respectively.
[b] TED, total energy distribution; ν, stretching; δ, bending; γ, out of plane bending; τ, torsion; ρ, scissoring.

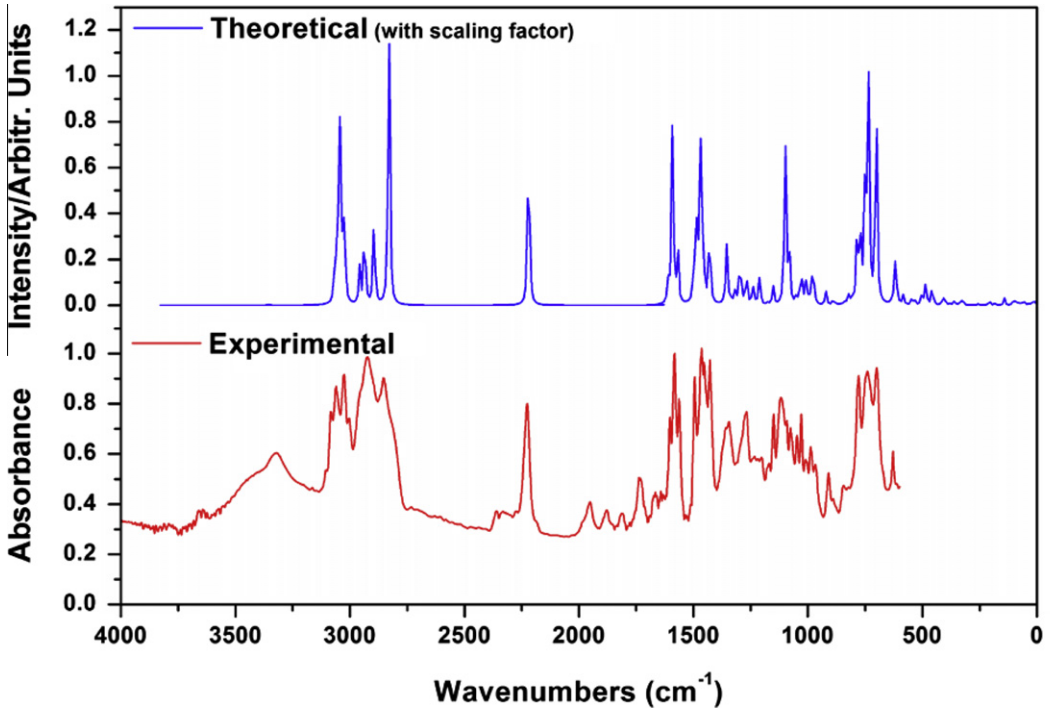

Fig. 2. The observed and calculated Infrared spectra of BPPPYA.

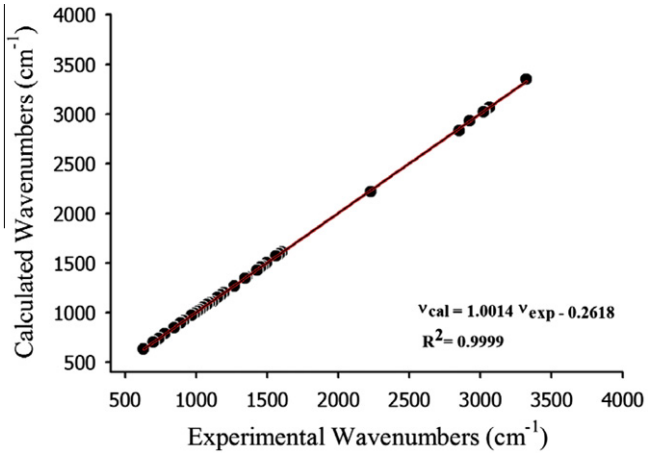

Fig. 3. Correlation graphics of calculated and experimental wavenumbers of BPPPYA.

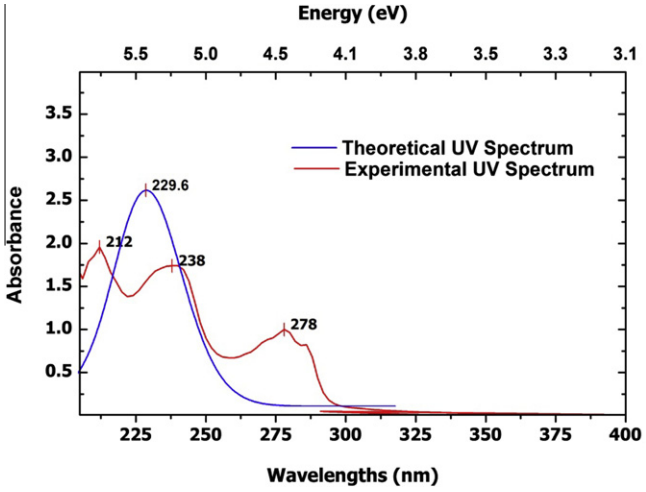

Fig. 4. The theoretical and experimental UV spectra of BPPPYA.

Table 3
Experimental and calculated by CIS approach wavelengths λ (nm), excitation energies (eV), oscillator strengths (f) in ethanol solution.

Experimental		Calculated (CIS)			Major contributes [a]	Assignments
λ (nm)	E (eV)	λ (nm)	E (eV)	f		
278	4.4388					$\pi-\pi^*$
238	5.1849	230	5.3871	0.6420	H-1 → L + 11 (11%), H → L + 11 (38%), H → L + 12 (21%)	$\pi-\pi^*$
212	5.8208	209	5.9288	0.0155	H-7 → L + 11 (17%), H-6 → L + 11 (11%)	$\pi-\pi^*$
		208	5.9449	0.0486	H-7 → L + 11 (12%), H → L + 17 (21%)	$\pi-\pi^*$

[a] H, HOMO; L, LUMO.

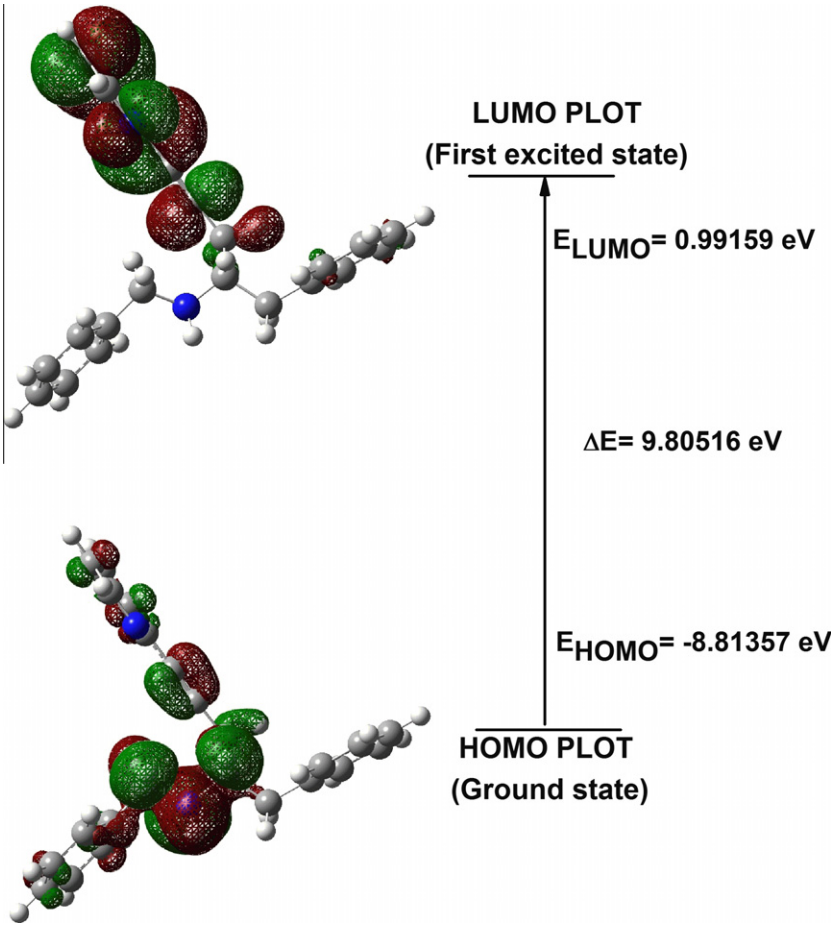

Fig. 5. The frontier molecular orbitals (HOMO and LUMO) for BPPPYA.

Table 4
Calculated energy values, chemical hardness, electronegativity, chemical potential, electrophilicity index and dipole moment of BPPPYA in solvent (ethanol).

B3LYP/6-311G++(d,p)	
E_{total} (Hartree)	−992.85898641
E_{HOMO} (eV)	−8.81357
E_{LUMO} (eV)	0.99159
$\Delta E_{HOMO-LUMO\ gap}$ (eV)	9.80516
E_{HOMO-1} (eV)	−9.10119
E_{LUMO+1} (eV)	1.15649
$\Delta E_{HOMO-1-LUMO+1\ gap}$ (eV)	10.25768
Chemical hardness (η)	4.90258
Electronegativity (χ)	3.91099
Chemical potential (μ)	−3.91099
Electrophilicity index (ω)	1.55998
Dipole moment (Debye)	1.46980

good coherent with the experimental data. Experimental and theoretical UV spectra of the BPPPYA are given in Fig. 4. Absorption maxima (λ_{max}; nm) for lower-lying singlet states of the molecule was calculated by CIS method. The theoretical and experimental maximum absorption wavelengths, excitation energies, absorbance and oscillator strengths are collected in Table 3. The spectrum illustrated three broad bands, a long wavelength band covering the 280–240 nm region and two of them covering the 240–200 nm region. Each of these bands corresponds to a number of overlapping transitions. The calculated visible absorptions which are functions of the electron availability were calculated at 208, 209 and 230 nm in ethanol solution by CIS approach. The absorption values were observed at 212 and 238 nm which are coherent with theoretical values.

The energy gap between the HOMOs and LUMOs is a critical parameter in determining molecular electrical transport properties because it is a measure of electron conductivity [58]. The energy gap difference calculations of the BPPPYA are illustrated in Fig. 5. Surfaces for the frontier orbitals were drawn to understand the reactivity scheme of the compound. According to Fig. 5, the HOMO of the compound presents a charge density localized mainly on the nitrogen atom located between rings and C≡C bond and LUMO is characterized by a charge distribution on wholly pyridine ring. The energy value of HOMO is computed at −8.81357 eV and LUMO is 0.99159 eV. The energy gap between HOMO and LUMO explains the chemical reactivity, optical polarizability, kinetic stability and chemical softness–hardness of a molecule. The chemical hardness is a good indicator of the chemical stability. The molecules having a small energy gap are known as soft and having a large energy gap are known as hard molecules. The hard molecules are not more polarizable than the soft ones because they need big energy to excitation [59]. Using the equation in the literature [60], the chemical potential, hardness and electrophilicity index have been calculated for BPPPYA and their values are shown in Table 4. In this study, the values of the chemical hardness and electronegativity were calculated at 4.90258 and 3.91099 eV, respectively. The value of energy gap between the HOMO and LUMO is 9.80516 eV and the value of hardness is 4.90258 eV for the title molecule. The chemical hardness value is a little bit smaller than that of (E)-4-methoxy-2-[(*p*-tolylimino)methyl]phenol molecule [23], which is a Schiff based compound (1.842 eV), that is a hardness molecule.

The TDOS, PDOS and overlap population(OPDOS or COOP) density of states [61–64], in terms of Mullikan population analysis were calculated and created by convoluting the molecular orbital information with Gaussian curves of unit height and Full Width

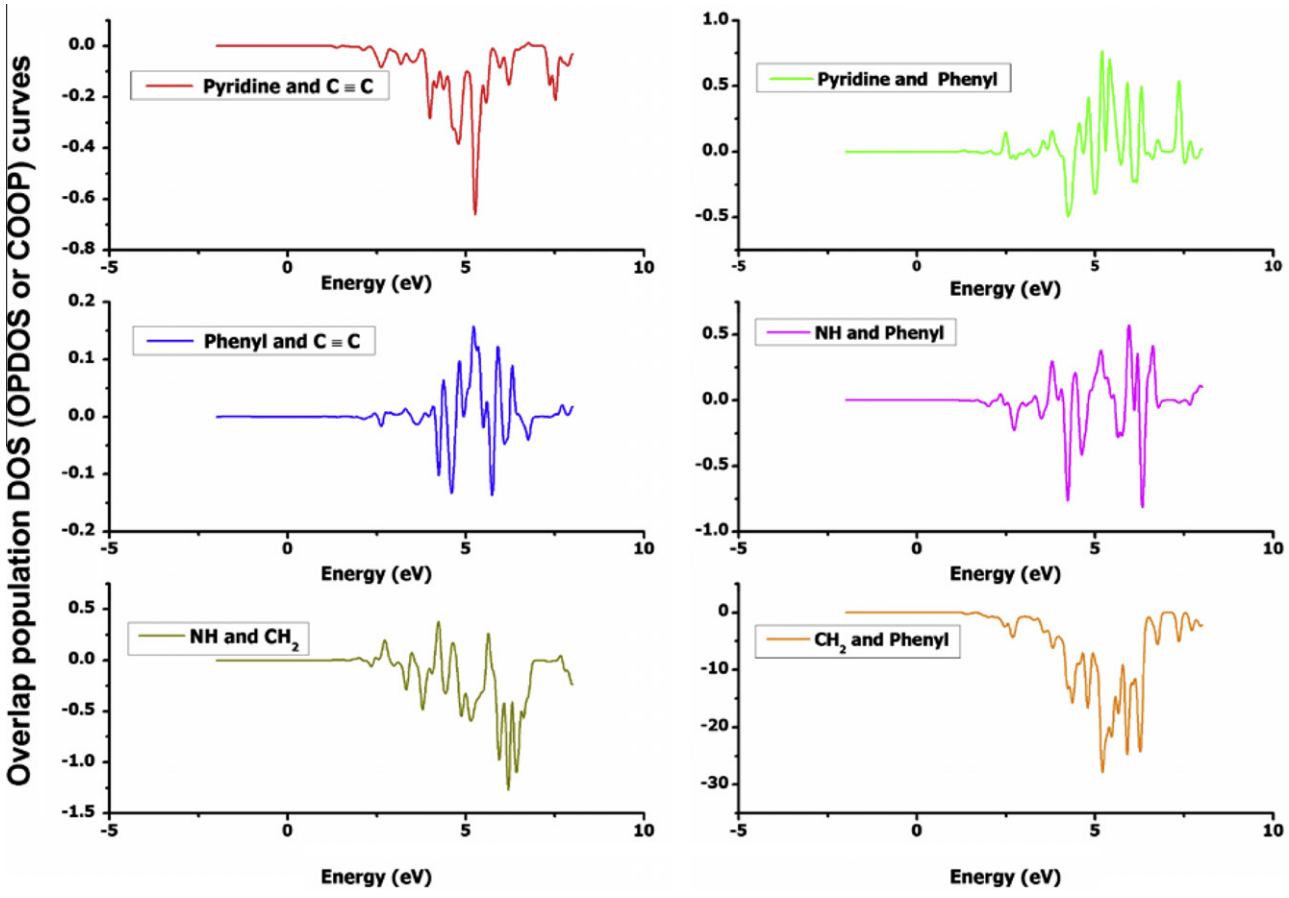

Fig. 6. Overlap population DOS (OPDOS or COOP) for BPPPYA.

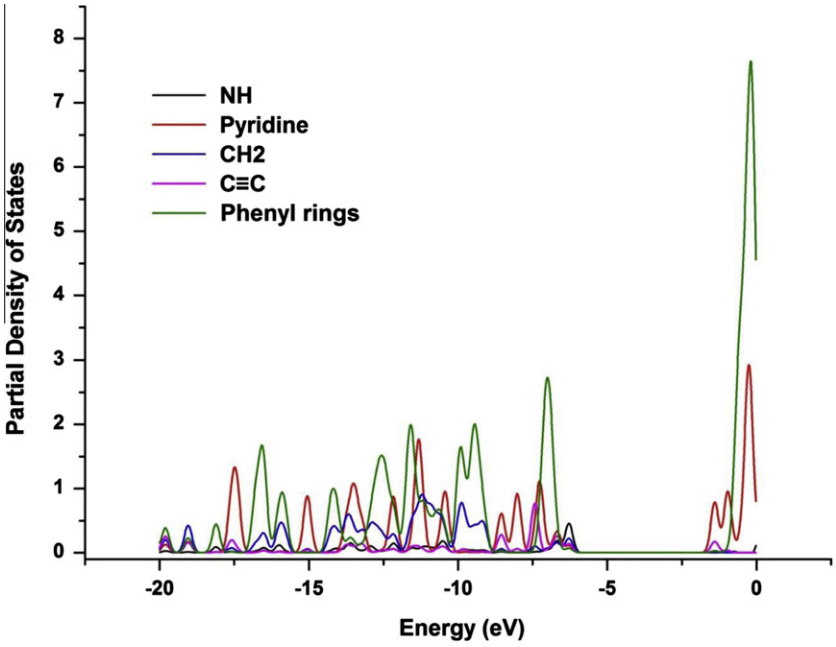

Fig. 7. Calculated partial electronic density of states (PDOS) for BPPPYA.

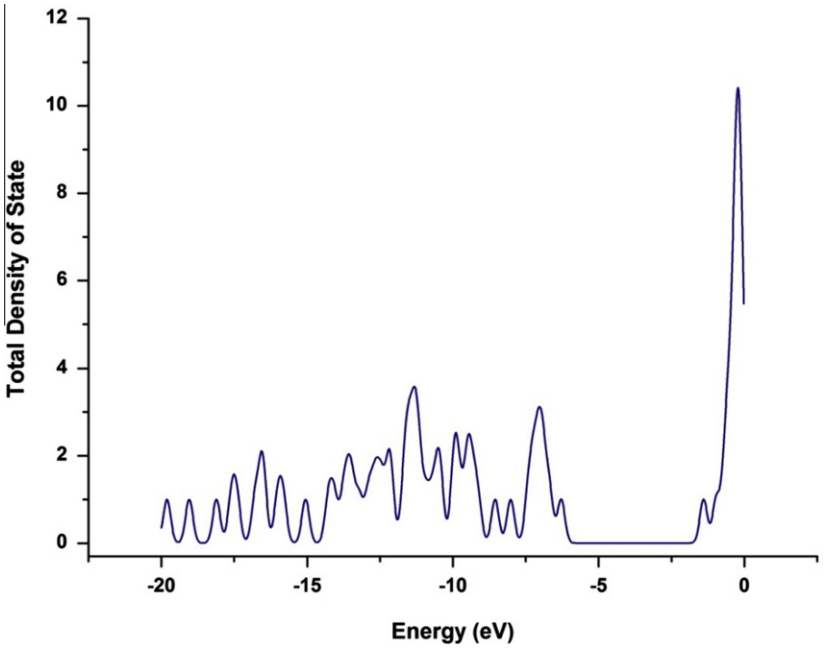

Fig. 8. Calculated total electronic density of states (TDOS) for BPPPYA.

at Half Maximum (FWHM) of 0.3 eV using Gausssum2.2 [61]. The Crystal Orbital Overlap Population (COOP), PDOS, and TDOS spectra were given in Fig. 6–8, respectively. The most important application of the DOS plots is to demonstrate molecule orbital (MO) compositions and their contributions to chemical bonding through the OPDOS plots which are also referred in the literature as (COOP) diagrams. The COOP is similar to DOS because it results from multiplying DOS by the overlap population. COOP shows the bonding, anti-bonding and nonbonding nature of the interaction of the two orbital's, atoms or groups. A positive value of the COOP indicates a bonding interaction, negative value means that there is an anti-bonding interaction and zero value indicates nonbonding interactions [65]. The PDOS mainly presents the composition of the fragment orbitals contributing to the molecular orbitals which is seen from Fig. 7. As seen Fig. 7 HOMO orbitals are localized on NH, CH_2, C≡C, pyridine and phenyl rings. The NH group orbitals play a significant role in HOMO orbitals and its contribution about 46%. The LUMO orbitals are localized on the pyridine rings (79%). In the electronic structure of the compound with pyridine the virtual molecular orbitals with large contribution of C≡C are LUMO 96% and LUMO+1 99%. Based on the percentage shares of atomic orbitals or molecular fragments in the molecule is difficult to compare

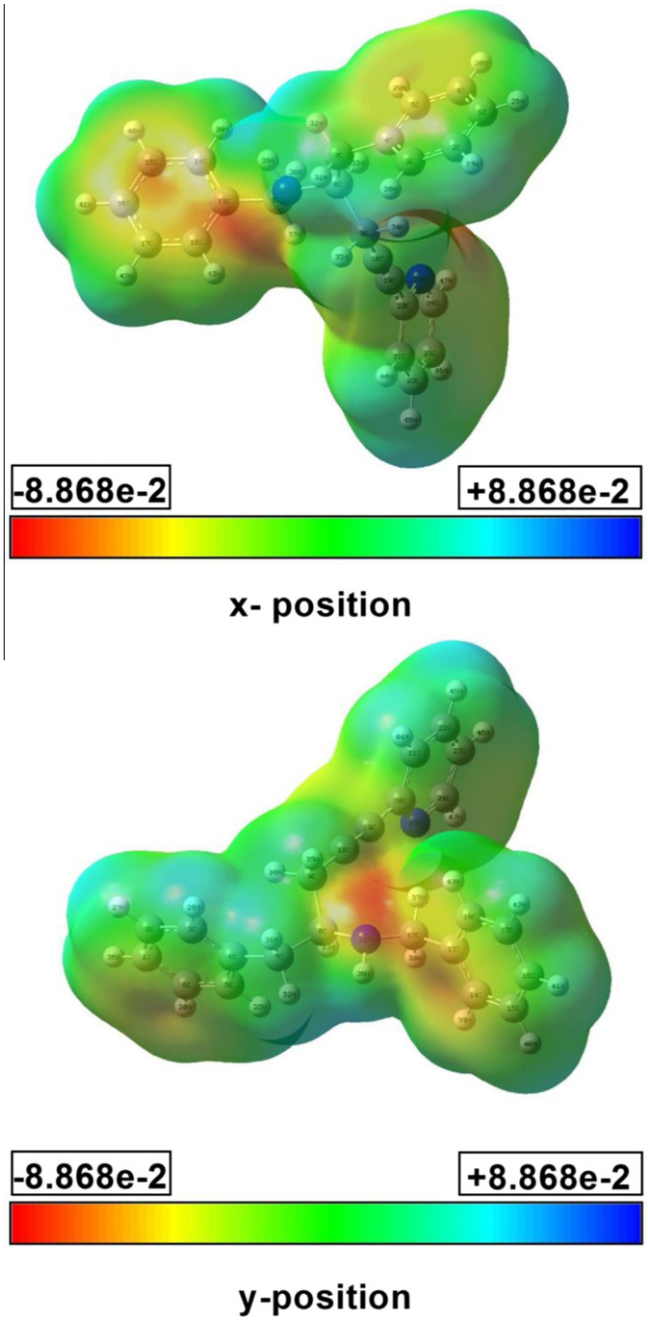

Fig. 9. Molecular electrostatic potential map (MEP) of BPPPYA.

groups in terms of its bonding and anti-bonding properties. The OPDOS diagram is shown Fig. 6 and some of orbitals of energy values of interaction between selected groups which are shown from Figs. 6 and 7, C≡C ↔ Pyridine (red line) system is negative (anti-bonding interaction) as well as CH_2 ↔ phenyl rings systems for the states in energy window about 1.27 to 7.99 eV. Nonbonding states are present for C≡C ↔ Pyrdine, CH_2 ↔ Phenyl rings and Phenyl ring ↔ C≡C, NH ↔ Phenyl rings, systems as well in the ranges of −2 to 1.21, −1.94 to 1.18, −1.95 to −4.9 (6.99 to 7.57) and −2 to 1.71 eV (6.92–7.57), respectively. As can be seen from the OPDOS diagram, the Phenyl ring ↔ C≡C, Pyridine ↔ Phenyl rings and Phenyl ring ↔ NH have significant bonding character which are of positive value and energy ranges 3.21 to 6.51, 2.40 to 7.64 and 2.34 to 6.72 eV is positive (bonding interactions), respectively.

One can see the OPDOS or COOP diagram, CH_2 ↔ phenyl rings (navy blue line) and C≡C ↔ pyridine (black line) system has the biggest intensity (negative anti-bonding interaction) as well as pyridine ↔ phenyl rings, C≡C ↔ phenyl rings, NH ↔ phenyl rings, NH ↔ CH_2 systems for the states in the energy window changes between negative and positive. Also it is worth mentioning that the OPDOS or COOP diagrams, the pyridine ↔ phenyl rings (bonding interactions), C≡C ↔ phenyl rings, NH ↔ phenyl rings, NH ↔ CH_2 have significant bonding character which have of positive values.

Molecular electrostatic potential (MEP) maps

To predict reactive sites for electrophilic and nucleophilic attack for the BPPPYA molecule, MEP was calculated at the B3LYP/6-311++G(d,p). The different values of the electrostatic potential at the surface are represented by different colors. Potential increases in the order red < orange < yellow < green < blue. The color code of these maps is in the range between −0.08868 a.u. (deepest red) to 0.08868 a.u. (deepest blue) in compound, where blue indicates the strongest attraction and red indicates the strongest repulsion. The positive regions of MEP were related to electrophilic reactivity and the negative regions to nucleophilic reactivity as shown in Fig. 9. As can be seen from the MEP map, the negative regions are mainly localized on the nitrogen atoms, N11 and N25. A maximum positive region is localized on the hydroxyl hydrogen atom indicating a possible site for nucleophilic attack. The negative potential value is −0.0866094 for N25 atom in pyridine ring. A maximum positive region localized on the H atom bond has value of 0.0511193 for H (belong to NH group). The MEP map shows that the negative potential sites are on electronegative atoms, the positive potential sites are around the hydrogen atom. From this results, we can say that the H atoms indicates the strongest attraction and N atom indicates the strongest repulsion.

NMR spectra and calculations

The experimental ^1H and ^{13}C NMR spectra of the BPPPYA are shown in Fig. 10a and b, respectively. The recorded and calculated ^1H and ^{13}C chemical shifts in chloroform ($CDCl_3$) solution are collected in Table 5. The atom statues were numbered according to Fig. 1. It is recognized that accurate predictions of molecular geometries are essential for reliable calculations of magnetic properties. Therefore, firstly, full geometry optimization of the BPPPYA was performed at the gradient corrected density functional level of theory using the hybrid B3LYP method based on Becke's three parameters functional of DFT. Then, GIAO ^1H and ^{13}C NMR chemical shift calculations of the compound was made by the same method using 6-311++G(d,p) basis set IEFPCM/$CDCl_3$ solution. Application of the GIAO [36] approach to molecular systems was significantly improved by an efficient application of the method to the ab initio SCF calculation, using techniques borrowed from analytic derivative methodologies. The isotropic shielding values were used to calculate the isotropic chemical shifts δ with respect to tetramethylsilane (TMS) $\delta^X_{iso} = \sigma^{TMS}_{iso} - \sigma^X_{150}$. The values of σ^{TMS}_{iso} is 182.46 ppm and 31.88 ppm for ^{13}C and ^1H NMR spectra, respectively.

As in Fig. 1, the studied compound has 23 different carbon atoms, which are 17 aromatic carbon signals calculated theoretically, while 13 aromatic carbon signals out of 17 aromatic carbons were observed experimentally in the ^{13}C NMR spectrum of the molecule, which arise the symmetry of two phenyl rings. In contrast to carbon signals, 22 proton signals were calculated while 21 protons were observed in the ^1H NMR spectrum according to integration. The N—H (H_{36}) proton signal calculated at 0.89 ppm is missing in the recorded spectrum. The H_{36} atom has the smallest shift in all chemical shifts and mostly localized on the periphery of

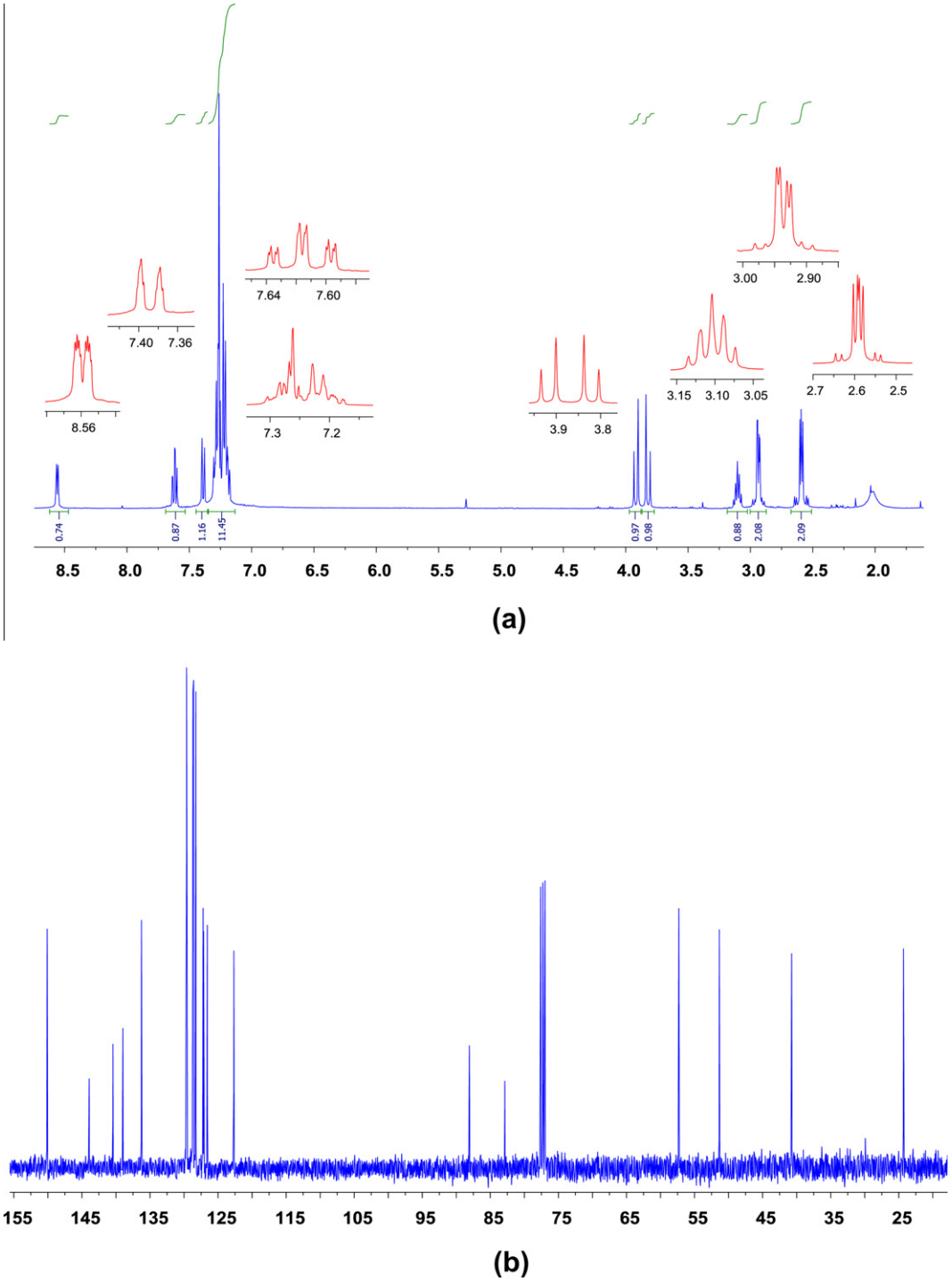

Fig. 10. (a) ^{1}H NMR (b) ^{13}C NMR spectra of BPPPYA.

molecules. Since the chemical shift is more susceptible to intermolecular interactions as compared other heavier atoms, the chemical shifts of the N—H varies greatly with concentration and solvent effects, and occasionally could not be seen in the ^{1}H NMR spectra [66].

Generally, the proton chemical shift of organic molecules varies greatly with the electronic environment of the proton. Hydrogen attached or nearby electron-withdrawing atom or group can decrease the shielding and move the resonance of attached proton towards to a higher frequency, whereas electron-donating atom or group increases the shielding and moves the resonance towards to a lower frequency [67]. The chemical shifts of aromatic protons of organic molecules are usually observed in the range of 7.00–8.00 ppm, while aliphatic protons resonance in the high field. The signals of the 14 aromatic proton of the title compound were calculated theoretically at 7.22–8.68 ppm, observed at 7.18–8.56 ppm experimentally. The chemical shift value of H_{47} (the nearest the nitrogen atom) is larger than the other proton signals due to the electronegative nature of nitrogen atom. We predicted H_{47} at 8.68 ppm in the lowest field, and H_{46} at 7.22 ppm in the highest field of the aromatic region. H_{45} is calculated at 7.68 ppm, observed at 7.62 ppm. Other 11 aromatic protons are accumulated in the

Table 5
Experimental and theoretical, ^{1}H and ^{13}C NMR isotropic chemical shifts (with respect to TMS and in $CDCl_3$ solution) of BPPPYA by DFT/B3LYP/6-311++G(d,p) method (atom positions were numbered as in Fig. 1).

Atoms	Carbon		Atoms	Hydrogen	
	Exp.	B3LYP		Exp.	B3LYP
C(1)	126.59–129.62	131.48	H(26)	7.18–7.30	7.50
C(2)	126.59–129.62	133.45	H(27)	7.18–7.30	7.61
C(3)	126.59–129.62	135.17	H(28)	7.18–7.30	7.35
C(4)	140.43	146.36	H(29)	7.18–7.30	7.68
C(5)	126.59–129.62	134.62	H(30)	7.18–7.30	7.61
C(6)	126.59–129.62	133.75	H(31)	2.91–2.96	2.36
C(7)	40.74	47.48	H(32)	2.91–2.96	2.80
C(8)	57.30	67.19	H(33)	3.10	3.31
C(9)	24.31	27.24	H(34)	2.56–2.62	2.64
C(10)	88.08	98.69	H(35)	2.56–2.62	2.29
C(12)	51.36	58.70	H(37)	3.92	4.65
C(13)	138.98	148.47	H(38)	3.82	3.77
C(14)	126.59–129.62	135.28	H(39)	7.18–7.30	7.50
C(15)	126.59–129.62	133.09	H(40)	7.18–7.30	7.61
C(16)	126.59–129.62	132.25	H(41)	7.18–7.30	7.50
C(17)	126.59–129.62	133.02	H(42)	7.18–7.30	7.50
C(18)	126.59–129.62	136.32	H(43)	7.18–7.30	7.87
C(19)	82.87	86.24	H(44)	7.18–7.30	7.50
C(20)	143.93	150.76	H(45)	7.62	7.68
C(21)	126.59–129.62	132.13	H(46)	7.39	7.22
C(22)	136.25	140.84	H(47)	8.56	8.68
C(23)	122.68	126.06			
C(24)	150.10	156.30			

Table 6
The electric dipole moment (D), polarizability and first hyperpolarizability of BPPPYA by DFT/B3LYP6-311++G(d,p).

	a.u.	esu ($\times10^{-24}$)		a.u.	esu ($\times10^{-33}$)
α_{xx}	410.744291	60.872304	β_{xxx}	−580.857754	−5018.204390
α_{xy}	−14.927840	−2.212306	β_{xxy}	546.825694	4724.191221
α_{yy}	383.378351	56.816672	β_{xyy}	−699.692087	−6044.849845
α_{xz}	4.296321	0.636715	β_{yyy}	1106.511455	9559.484416
α_{yz}	9.473434	1.403963	β_{xxz}	221.085874	1910.027195
α_{zz}	383.113104	56.777362	β_{xyz}	−56.301750	−486.407707
α_{tot}	392.411915	58.155446	β_{yyz}	91.110719	787.132831
$\Delta\alpha$	711.961264	105.512659	β_{xzz}	13.122571	113.369825
μ_x	−0.199302		β_{yzz}	−39.611752	−342.217806
μ_y	0.207131		β_{zzz}	9.998986	86.384239
μ_z	−0.438539		β_x	−1267.427270	−10949.684409
μ	0.524348		β_y	1613.725398	13941.457830
			β_z	322.195579	2783.544265
			β_{tot}	2077.087272	17944.580067

range of 7.50–7.87 ppm, observed experimentally in 7.18–7.30 ppm, showed good correlation with theoretical data.

The aliphatic 7 protons were calculated in the region of 2.29–4.65 ppm, observed in 2.56–3.92 ppm. Benzylic protons were predicted 4.65 (H_{37}) and 3.77 (H_{38}) ppm, observed as doublets at 3.92 and 3.82 ppm, respectively. Methyne proton (H_{33}) was calculated at 3.31 ppm, observed as quintet at 3.10 ppm. Methylene protons (H_{31}, H_{32}) of the molecule were predicted at 2.36 and 2.80 ppm and observed as two different doublet of doublets at 2.91 and 2.96 ppm, respectively. The other methylene protons (H_{34}, H_{35}) next to the triple bond were calculated at 2.64 ppm and 2.29 ppm, respectively, while observed as two different doublet of doublets at 2.56 and 2.62 ppm. Overall, the calculated protons chemical shifts of the molecule show fairly good correlation to the experimental spectrum.

Aromatic carbons give signals in overlapped areas of the spectrum with chemical shift values ranging from 100 to 150 ppm [66–68]. The 17 aromatic carbons were calculated at 122.68–150.10 ppm theoretically, observed signals are in the range of

Table 7
Mulliken atomic charges of BPPPYA.

C1	−0.417467	H26	0.179459
C2	−0.344575	H27	0.204311
C3	−0.434700	H28	0.185137
C4	0.817909	H29	0.190348
C5	−0.096867	H30	0.201784
C6	−0.302332	H31	0.202138
C7	−0.449172	H32	0.198396
C8	−0.060585	H33	0.154941
C9	−0.490092	H34	0.175712
C10	−0.045797	H35	0.209202
C12	−0.986245	H36	0.217077
C13	0.791664	H37	0.065332
C14	−0.105303	H38	0.125822
C15	−0.459355	H39	0.199347
C16	−0.322645	H40	0.196521
C17	−0.250936	H41	0.185842
C18	−0.031255	H42	0.197867
C19	0.182510	H43	0.191961
C20	−0.671739	H44	0.230807
C21	0.117536	H45	0.211614
C22	−0.511786	H46	0.215299
C23	−0.000702	H47	0.203744
C24	−0.130770	N11	0.092413
		N25	−0.032365

126.06–156.30 ppm. It is worth mentioned that the aromatic carbon chemical shifts (*ipso*-carbons C_4, C_{13}) is calculated at 146.36 and 148.47 ppm, observed at 140.43 and 138.98 ppm. As the pyridine ring, N25 atom exhibits electronegative property, the experimental chemical shift values of C_{24} (150.1 ppm) and C_{20} (143.93 ppm) which calculated at 156.30 and 150.76 ppm are larger than other carbons chemical shifts values (C_{21}, C_{22} and C_{23}) (see Table 5). The lowest signal of the aromatic carbons atom C_{23} was predicted at 126.06 ppm and observed at 122.68 ppm. The other phenyl and pyridine ring carbon chemical shifts (14 aromatic carbons) were observed in the range of 126.59–129.62 ppm and calculated at the range of 131.48–136.32 ppm, showing a good correlation as seen in Table 5.

Aliphatic carbons were observed in the region of 20–90 ppm. Triple bond carbons resonanced at 88.08 (C_{10}) and 82.87 ppm (C_{19}) and the chemical shifts of these carbons were calculated at 98.69 and 86.24 ppm, respectively. Methyne and methylenes carbons were calculated at 67.19 (C_8), 58.70 (C_{12}), 47.48 (C_7) and 27.24 (C_9) using by the B3LYP method and observed at 57.30, 51.36, 40.74 and 24.31 ppm, respectively. The ^{1}H and ^{13}C chemical shifts data show suitability with the predicted values, and described fairly well by the selected DFT method combined with the basis set.

Nonlinear optical (NLO) effects

Some new materials show efficient nonlinear optical features, therefore, NLO properties has been of great interest by the recent years. In this study, the electronic dipole moment, molecular polarizability, anisotropy of polarizability and molecular first hyperpolarizability of present compound were investigated. The polarizability and hyperpolarizability tensors (α_{xx}, α_{xy}, α_{yy}, α_{xz}, α_{yz}, α_{zz} and β_{xxx}, β_{xxy}, β_{xyy}, β_{yyy}, β_{xxz}, β_{xyz}, β_{yyz}, β_{xzz}, β_{yzz}, β_{zzz}) can be obtained by a frequency job output file of Gaussian. However, α and β values of Gaussian output are in atomic units (a.u.) so they have been converted into electronic units (esu) (α; 1 a.u. = 0.1482×10^{-24} esu, β; 1 a.u. = 8.6393×10^{-33} esu). The mean polarizability (α), anisotropy of polarizability ($\Delta\alpha$) and the average value of the first hyperpolarizability $\langle\beta\rangle$ can be calculated using the equations.

$$\alpha_{tot} = \frac{1}{3}(\alpha_{xx} + \alpha_{yy} + \alpha_{zz})$$

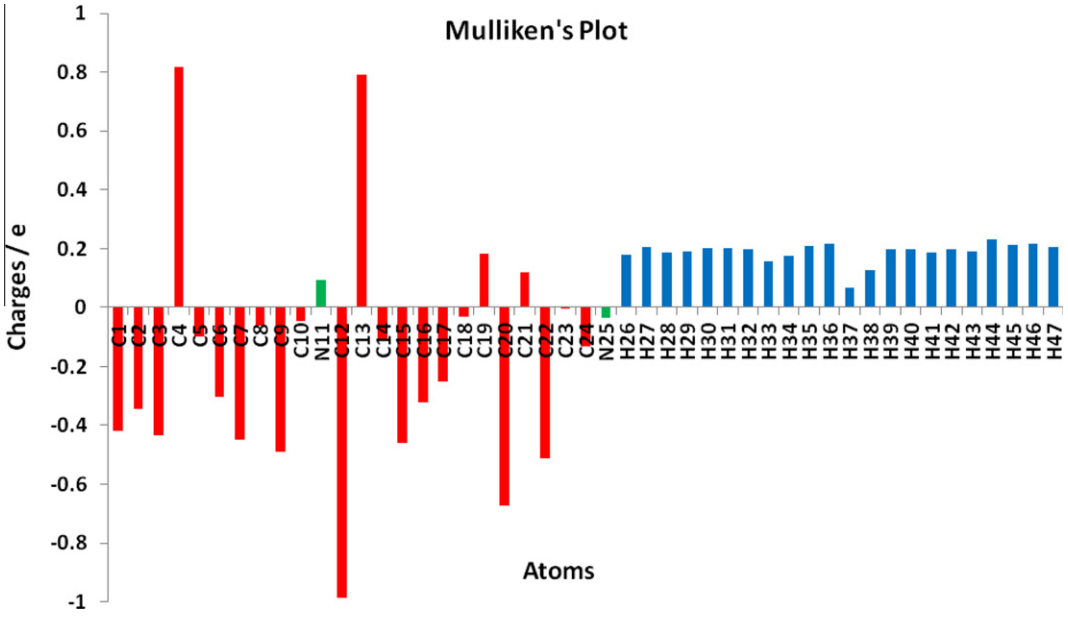

Fig. 11. Mulliken atomic charge distribution of BPPPYA.

$$\Delta\alpha = \frac{1}{\sqrt{2}}\left[(\alpha_{xx}-\alpha_{yy})^2+(\alpha_{yy}-\alpha_{zz})^2+(\alpha_{zz}-\alpha_{xx})^2 + 6\alpha_{xz}^2+6\alpha_{xy}^2+6\alpha_{yz}^2\right]^{\frac{1}{2}}$$

$$\langle\beta\rangle = \left[(\beta_{xxx}+\beta_{xyy}+\beta_{xzz})^2+(\beta_{yyy}+\beta_{yzz}+\beta_{yxx})^2 + (\beta_{zzz}+\beta_{zxx}+\beta_{zyy})^2\right]^{\frac{1}{2}}$$

In Table 6, the calculated parameters described above and electronic dipole moment {μ_i ($i = x, y, z$) and total dipole moment μ_{tot}} for title compound are listed. The total dipole moment can be calculated using the following equation.

$$\mu_{tot} = (\mu_x^2+\mu_y^2+\mu_z^2)^{\frac{1}{2}}$$

It is well known that the higher values of dipole moment, molecular polarizability, and hyperpolarizability are important for more active NLO properties. The calculated dipole moment is equal to 0.524348 Debye (D). The highest value of dipole moment is observed for component μ_z. In this direction, this value is equal to 0.438539 D. The calculated polarizability α_{ij} have non-zero values and was dominated by the diagonal components. Total polarizability (α_{tot}) and anisotropy of polarizability ($\Delta\alpha$) are calculated as $58.155446 \times 10^{-24}$ esu and $105.512659 \times 10^{-24}$ esu. The first hyperpolarizability value β_{tot} of the title compound is equal to $179.44580067 \times 10^{-31}$ esu^{-1}. The hyperpolarizability β dominated by the longitudinal components of β_{xxx}. Domination of particular component indicates on a substantial delocalization of charges in this direction.

The polarizability and the first hyperpolarizability of title molecule is ca. 11 and 22 times greater than those of urea (α and β of urea are 9.868774×10^{-24}, and 7.803240×10^{-31} cm^5 esu^{-1} obtained by B3LYP/6-311++G(d,p) method). That is to say, the title compound can be used as a good candidate of NLO materials.

Mulliken atomic charges

The computed of reactive atomic charges plays an important role in the application of quantum mechanical calculations the molecular system. The Mulliken atomic charges of title molecule is presented in Table 7 and shown in Fig. 11. The Mulliken atomic charges are computed by the DFT/B3LYP method 6-311++G(d,p) basis set.

As can be seen in Table 7, all hydrogen atoms and N11 atom have a net positive charge however, the N25. The negative charge located on N25 atom which is donor atom and net positive charge on hydrogen atoms, which are acceptor atoms. The donor and acceptor atoms may suggest the presence of both inter-molecular hydrogen bonding in the crystalline phase.

Conclusions

In this work, (*S*)-*N*-Benzyl-1-phenyl-5-(pyridin-2-yl)-pent-4-yn-2-amine, was synthesized for the first time and several properties were studied using experimental techniques (FT-IR, NMR and UV) and tools derived from the density functional theory. The vibrational FT-IR spectrum of molecule was recorded and vibrational modes were assigned with aid of the experimental and computed vibrational wavenumbers and their TED. The magnetic properties of title compound were observed and calculated, and compared with experimental data. The TDOS, PDOS and OPDOS diagrams were plotted. The electronic properties were also calculated and experimental electronic spectrum was recorded with help of UV spectrometer. The comparisons of the predicted bands are generally in good agreement with experimental results. Furthermore, the polarizability, first hyperpolarizability and total dipole moment of title molecule were calculated and the results were discussed. These results indicate that the studied compound is a good candidate of nonlinear optical materials. We hope that the results of this study will help researchers to synthesis new materials.

Acknowledgement

This work was supported by the Celal Bayar University Research fund through research Grant No.: FBE-2008/54 and FEF-2009/101.

Appendix A. Supplementary data

Supplementary data associated with this article can be found, in the online version, at http://dx.doi.org/10.1016/j.saa.2012.06.041.

References

[1] T.L. Gilchrist, Heterocylic Chemistry, John Wiley & Sons Inc., New York, 1988.
[2] J.A. Fallas, L. Gonzalez, I. Corral, J. Tetrahedron Lett. 65 (2009) 232–236.
[3] F. Zucchi, G. Trabanelli, N.A. Gonzalez, J. Arch. Modern Chem. 132 (1995) 4579–4584.
[4] W. Liaw, N. Lee, C. Chen, C. Lee, G. Lee, S. Peng, J. Am. Chem. Soc. 122 (2000) 488–492.
[5] K.Y. Rajpure, C.H. Bhosale, J. Matrix Chem. Phys. 64 (2000) 70–76.
[6] S. Licht, J. Sol. Energy Mat. Solar Cells 38 (1995) 305–310.
[7] S.P. Jose, S. Mohan, Spectrochim. Acta 64A (2006) 240–245.
[8] K. Othmer, Encyclopedia of Chemical Technology, fourth ed., vol. 20, 1997.
[9] P. Pierrat, P.C. Gros, Y. Fort, J. Comb. Chem. 7 (2005) 879–886.
[10] M. Karabacak, E. Sahin, M. Cinar, I. Erol, M. Kurt, J. Mol. Struct. 886 (2008) 148–157.
[11] G. Rauhut, P. Pulay, J. Phys. Chem. 99 (1995) 3093–3100.
[12] N. Sundaraganesan, S. Ilakiamani, H. Saleem, P.M. Wojciechowski, D. Michalska, Spectrochim. Acta A 61 (2005) 2995–3001.
[13] M. Karabacak, A. Coruh, M. Kurt, J. Mol. Struct. 892 (2008) 125–131.
[14] S. Yurdakul, M. Yurdakul, J. Mol. Struct. 834–836 (2007) 555–560.
[15] N. Sundaraganesan, C. Meganathan, B. Ananda, B. Dominic Joshua, Christine Lapouge, Spectrochim. Acta Part A 67 (2007) 830–836.
[16] A. Topacli, S. Bayari, Spectrochim. Acta A 57 (2001) 1385–1389.
[17] R.N. Medhi, R. Barman, K.C. Medhi, S.S. Jois, Spectrochim. Acta A 56 (2000) 1523–1528.
[18] I. Lopez Tocon, M.S. Wooley, J.C. Otero, J.I. Marcos, J. Mol. Struct. 470 (1998) 241–246.
[19] J.M.L. Martin, C. Van Alsenoy, J. Phys. Chem. 100 (1996) 6973–6983.
[20] G. Zerbi, B. Crawford, J. Overend, J. Chem. Phys. 38 (1963) 122–127.
[21] Z. Meng, W.R. Carper, J. Mol. Struct. (THEOCHEM) 588 (2002) 45–53.
[22] A. Atac, M. Karabacak, C. Karaca, E. Kose, Spectrochim. Acta A 85 (2012) 145–154.
[23] A.M. Asiri, M. Karabacak, M. Kurt, K.A. Alamry, Spectrochim. Acta A 82 (2011) 444–455.
[24] A. Coruh, F. Yilmaz, B. Sengez, M. Kurt, M. Cinar, M. Karabacak, Struct. Chem. 22 (2011) 45–56.
[25] M. Eskici, A. Karanfil, M.S. Ozer, C. Sarıkurkcu, Tetrahedron Lett. 52 (2011) 6336–6341.
[26] P. Hohenberg, W. Kohn, Phys. Rev. 136 (1964) B864–B871.
[27] A.D. Becke, J. Chem. Phys. 98 (1993) 5648–5652.
[28] C. Lee, W. Yang, R.G. Parr, Phys. Rev. B 37 (1988) 785–789.
[29] M.J. Frisch et al., GAUSSIAN 09, Revision A.1, Gaussian, Inc., Wallingford, CT, 2009.
[30] A.J. Williams, S. Chaktong, S. Gray, R.M. Lawrence, T. Gallegher, Org. Lett. 5 (2003) 811–814.
[31] H.B. Schlegel, J. Comput. Chem. 3 (1982) 214–218.
[32] M. Karabacak, M. Cinar, A. Coruh, M. Kurt, J. Mol. Struct. 919 (2009) 26–33.
[33] M. Karabacak, M. Kurt, M. Cinar, A. Coruh, Mol. Phys. 107 (3) (2009) 253–269.
[34] M. Karabacak, M. Cinar, S. Ermec, M. Kurt, J. Raman Spectrosc. 41 (2010) 98–105.
[35] J. Baker, A.A. Jarzecki, P. Pulay, J. Phys. Chem. A102 (1998) 1412–1424.
[36] R. Ditchfield, J. Chem. Phys. 56 (1972) 5688–5691.
[37] K. Wolinski, J.F. Hinton, P. Pulay, J. Am. Chem. Soc. 112 (1990) 8251–8260.
[38] M. Petersilka, U.J. Gossmann, E.K.U. Gross, Phys. Rev. Lett. 76 (1966) 1212–1215.
[39] R. Bauernschmitt, R. Ahlrichs, Chem. Phys. Lett. 256 (1996) 454–464.
[40] M. Cinar, A. Coruh, M. Karabacak, Spectrochim. Acta A 83 (2011) 561–569.
[41] T.W. Hambley, H.K. Chan, I. Gonda, J. Am. Chem. Soc. 108 (1986) 2103–2105.
[42] M. Nethaji, V. Pattabhi, G.R. Desiraju, Acta Cryst. C 44 (1988) 275–277.
[43] S. LoÈhr, M. Yonemura, A. Orita, N. Imai, H. Akashi, J. Otera, Acta Cryst. E59 (2003) 594–595.
[44] V.K. Rastogi, M.A. Palafox, R.P. Tanwar, L. Mittal, Spectrochim. Acta A 58 (2002) 1989–1997.
[45] M. Silverstein, G. Clayton Basseler, C. Morill, Spectrometric Identification of Organic Compounds, Wiley, New York, 1981.
[46] J. Coates, R.A. Meyers, Interpretation of Infrared Spectra: A Practical Approach, John Wiley and Sons Ltd., Chichester, 2000.
[47] J.P. Abraham, I.H. Joe, V. George, O.F. Nielson, V.S. Jayakumar, Spectrochim. Acta 59A (2003) 193–199.
[48] D. Lin-Vien, N.B. Colthup, W.G. Fateley, J.G. Grasselli, The Handbook of Infrared and Raman Characteristic Frequencies of Organic Molecules, Academic Press, Boston, MA, 1991.
[49] G. Varsanyi, Assignments of Vibrational Spectra of Seven Hundred Benzene Derivatives, vol. 1–2, Adam Hilger, 1974.
[50] D. Sajan, L. Joseph, N. Vijayan, M. Karabacak, Spectrochim. Acta A 81 (2011) 85–98.
[51] L.J. Bellamy, The Infrared Spectra of Complex Molecules, vol. 2, Chapman and Hall, London, 1980.
[52] N.B. Colthup, J. Opt. Soc. Am. 40 (1950) 397–400.
[53] J.E. Stewart, J. Chem. Phys. 30 (1959) 1259.
[54] M. Karabacak, M. Kurt, Spectrochim. Acta A 71 (2008) 876–883.
[55] M. Kumar, S. Jaiswal, R. Singh, G. Srivastav, P. Singh, T.N. Yadav, R.A. Yadav, Spectrochim. Acta A 75 (2010) 281–292.
[56] J.L.H. Allan, G.O. Meakins, M.C. Whiting, J. Chem. Soc. (1955) 1874–1881.
[57] L.J. Bellamy, Advances in Infrared group Frequencies, Methuen, London, 1968.
[58] N. Sundaraganesan, B.D. Joshua, K. Settu, Spectrochim. Acta A 66 (2007) 381–388.
[59] R.G. Pearson, Proc. Natl. Acad. Sci. USA 83 (1986) 8440–8841.
[60] V. Thanikachalam, V. Periyanayagasamy, J. Jayabharathi, G. Manikandan, H. Saleem, S. Subashchandrabose, Y. Erdogdu, Spectrochim. Acta A 87 (2012) 86–95.
[61] R. Hoffmann, Solids and Surfaces: A Chemist's View of Bonding in Extended Structures, VCH Publishers, New York, 1988.
[62] T. Hughbanks, R. Hoffmann, J. Am. Chem. Soc. 105 (1983) 3528–3537.
[63] J.G. Malecki, Polyhedron 29 (2010) 1973–1979.
[64] N.M. O'Boyle, A.L. Tenderholt, K.M. Langner, J. Comp. Chem. 29 (2008) 839–845.
[65] M. Chen, U.V. Waghmare, C.M. Friend, E. Kaxiras, J. Chem. Phys. 109 (1998) 6680–6854.
[66] K. Pihlaja, E. Kleinpeter, Carbon−13 Chemical Shifts in Structural and Stereo Chemical Analysis, VCH Publishers, Deerfield Beach, FL, 1994.
[67] N. Subramania, N. Sundaraganesan, J. Jayabharathi, Spectrochim. Acta A 76 (2010) 259–269.
[68] H.O. Kalinowski, S. Berger, S. Braun, ^{13}C NMR Spectroscopy, John Wiley & Sons, Chichester, 1988.